



Published in final edited form as:

*Am J Hematol.* 2012 December ; 87(12): 1057–1064. doi:10.1002/ajh.23317.

## Synergistic antiproliferative effects of arsenic trioxide (ATO) with bortezomib in mantle cell lymphoma (MCL)

Hyun Joo Jung, MD<sup>1,2</sup>, Zheng Chen<sup>1</sup>, and Nami McCarty, PhD<sup>\*1</sup>

<sup>1</sup>Centre for Stem Cell Research, Brown Foundation Institute of Molecular Medicine for the Prevention of Human Diseases (IMM) University of Texas-Health Science Center at Houston, Houston, Texas, USA

<sup>2</sup>Division of Hematology-Oncology, Department of Pediatrics, Ajou University Hospital, Ajou University School of Medicine, Suwon, Korea

### Abstract

Mantle cell lymphoma (MCL) is a subtype of B-cell Non-Hodgkin's Lymphoma (NHL) and accounts for approximately 6% of all lymphomas. MCL is highly refractory to most chemotherapy including newer antibody-based therapeutic approaches, and high-grade MCL has one of the worst survival rates among NHLs. Therefore, the development of new therapeutic strategies to overcome drug resistance of MCL is important. In this article, we tested the effects of arsenic trioxide (As<sub>2</sub>O<sub>3</sub>, ATO) in bortezomib-resistant MCL. ATO is reported to induce complete remission in the patients with relapsed or refractory acute promyelocytic leukemia. Their effects in MCL, however, have not been explored. We show here that ATO effectively inhibited the growth of MCL cells by reducing NF-κB expression. The induction of apoptosis in MCL was partially due to reduced levels of cyclin D1 and increased levels of apoptosis-related molecules. The antiproliferative effects of bortezomib on MCL greatly increased when the cells were also treated with ATO, indicating ATO can sensitize MCL to bortezomib. Similar results were noted in bortezomib-resistant cell lines. In conclusion, ATO may be an alternative drug for use in combined adjuvant therapies for MCL, and further clinical testing should be performed.

### Keywords

Mantle cell lymphoma; Arsenic trioxide; Bortezomib; Antineoplastic drug resistance; Non-Hodgkin's Lymphoma

### INTRODUCTION

Mantle cell lymphoma (MCL) is a subtype of non-Hodgkin's lymphoma (NHL), the sixth most common type of human cancer in the United States [1,2]. MCLs display widespread cellular heterogeneity and are resistant to standard chemotherapeutic interventions. As a result, the median survival time for patients with malignant MCL is less than three years, and these patients have the worst survival rate among NHLs [2,3].

\*Correspondence: Nami McCarty, University of Texas-Health Science Center at Houston, 1835 Pressler St., IMM-630F, Houston, TX 77030, USA. nami.mccarty@uth.tmc.edu, Tel: 713-500-2495, Fax: 713-500-2424.

#### AUTHOR CONTRIBUTIONS

HJJ performed and analyzed experiments and wrote the manuscript. ZC performed experiments. NM supervised overall research, and wrote the manuscript.

To develop new therapeutic approaches that can increase patient survival, we tested arsenic trioxide ( $\text{As}_2\text{O}_3$ , ATO), a therapeutic agent used for thousands of years in traditional medicine [4,5]. Recently, ATO was successfully shown to induce a prolonged remission in patients with Acute Promyelocytic Leukemia (APL), especially at low concentrations [6,7]. ATO also has been tested in Multiple Myeloma (MM) both as a single agent and in combination therapy in patients with advanced disease [8]. The clinical responses obtained after two months of therapy lasted approximately 6 weeks [9,10]. The limited clinical response of ATO in MM is likely due to the nature of compounds combined with ATO. Given that ATO targets many different pathways [11,12], ATO could also be a good therapeutic candidate for a complex disease such as MCL.

Enhancing pro-apoptotic pathways is one of the most well-characterized mechanisms of action for ATO. In myeloid leukemia cells, ATO can induce cell death by the activation of caspases followed by the inactivation of poly(ADP-ribose)polymerase (PARP) [13], an enzyme involved in DNA repair and genome maintenance [14]. In several lymphoid malignancy cell lines, ATO was reported to induce apoptosis by down-regulating Bcl-2 expression [15]. There are, however, no preclinical studies that used ATO as a therapeutic agent in MCL patients or that focused on understanding the mechanisms of action for ATO-induced cell death in MCL.

We report here ATO induces apoptosis in MCL via increasing the expression of caspase 3/9 and reducing that of Bcl-2. The increased levels of caspase 3/9 then induced the cleavage of PARP. ATO also decreased the expression levels of cyclin D1 and the survival factor NF- $\kappa$ B in MCL. NF- $\kappa$ B-related pathways were reported to be important for the selective survival of both MCL stem cells and MCL cells [16,17]. Therefore, the reduction of NF- $\kappa$ B signaling by ATO has important clinical implications.

ATO synergized the antiproliferative action of bortezomib in MCL. In the bortezomib-sensitive cell lines, Jeko-1 and SP-53, ATO increased the antiproliferative function of bortezomib. In addition, the combination of bortezomib and ATO had higher cytotoxic effects in Mino and REC-1 cell lines, which have been reported to be bortezomib-resistant [18].

## MATERIALS AND METHODS

### Patient samples and cell lines

Blood specimens from MCL patients were obtained after informed consents, as approved by M.D. Anderson Cancer Center as well as by the University of Texas-Health Science Center Institutional Review Boards. Tumor cells were harvested via aphaeresis from patients with clinically confirmed stage 4 MCL, with involvement of extra nodal sites such as the intestinal tract, kidney, bone marrow and peripheral blood. In each sample, markedly increased numbers of committed B cells (CD19+CD20+) were present compared to normal PBMC samples [19]. At the time of diagnosis each sample was positive for the t(11:14) (q13;q32) translocation, as determined by FISH [19]. We also confirmed elevated levels of cyclin D1 gene expression in all patient samples by real-time PCR [19]. The patients were previously treated, although the course of therapy differed somewhat between patients. Well-characterized Epstein-Barr virus-negative human MCL cell lines, Jeko-1, SP-53, Mino and REC-1 were obtained from ATCC (Manassas, VA).

### Cell preparation and culture

The primary MCL cells were cultured in complete RPMI 1640 (Cellgro, Manassas, VA) media, which contained 10% heat-inactivated fetal bovine serum (FBS), 2 mM glutamine, 100  $\mu$ g/ml streptomycin and 100  $\mu$ g/ml penicillin. Jeko-1 and SP-53 were cultured in the

same RPMI 1640 medium as stated above, and RPMI 1640 (ATCC, Manassas, VA) medium, which contained 20% heat-inactivated FBS, 100 µg/ml streptomycin and 100 µg/ml penicillin was used for Mino and REC-1.

## Reagents

The commercially available antibodies were used; anti-CD45 (HI30, IgG1, K), anti-CD19 (HIB19, IgG1, K), anti-CD3 (HIT3a, IgG2a, K), anti-CD34 (581, IgG1, K), anti-cyclin D1 (ab61758, Abcam), anti-Bcl-2 (ab32124, Abcam), anti-cleaved PARP (Asp214, Cell Signaling), cleaved caspase-9 (Asp315, Cell signaling), cleaved caspase-3 (Asp175, Cell signaling). All antibodies were purified or conjugated with appropriate fluorochromes based on the combinations of antibodies used in each experiment. All chemotherapeutic drugs were obtained from the pharmacy at M.D. Anderson Cancer Center. We used the drug concentrations which were determined in our previous paper [17], which was based on our preliminary data using MCL tumor samples as well as the concentrations reported in various studies on human hematological malignancies.

## Flow cytometry

After culture with different concentrations of ATO, the cells were stained by 7-Amino-Actinomycin (7-AAD) (BD Pharmingen™, San Diego, CA) and Fluorescein isothiocyanate (FITC)-labeled anti-Annexin V (BD Pharmingen™, San Diego, CA), and then analyzed using FACS LSRII flow cytometer (BD Biosciences). All assays were performed in duplicate.

## Immunohistochemical analysis

Suspended cells were added to the coated glass slide and fixed in cold acetone for 5 min at room temperature. Fixed cells were incubated with the primary antibodies overnight. Slides were washed and incubated with biotinylated secondary antibodies (Dako). Signals were detected after incubating slides with ABC complex (Vector lab) followed by incubation with DAB (Vector). Counterstaining was done with Mayer's Hematoxylin (Sigma) for 10 min at RT. Slides will be dehydrated before pictures were taken.

## Enzyme-linked immunosorbent assay (ELISA)

To prepare nuclear extracts,  $1 \times 10^6$  cells were washed with cold phosphate buffered saline (PBS)/Phosphatase Inhibitors, and harvested with 100 µl  $1 \times$  hypotonic buffer on ice. Nuclei were separated by centrifugation, and resuspended in 10 µl complete lysis buffer. After 30 min of incubation on ice, nuclear lysates were collected by high speed centrifugation. The buffers were purchased from Active Motif, and all steps were performed according to the manufacturer's instructions. 5 µg of nuclear extracts were used to assay for the NF-KB p50 and p65 DNA-binding activity using ELISA-based assay, according to the protocol of Active Motif TransAM™ NFKB Family Kit. Briefly, NF-KB oligonucleotide (5'-GGGACTTTCC-3')-coated 96-well plate was incubated with nuclear extracts indicated above. The primary Abs used to detect NF-KB that recognizes an epitope on p50 and p65. HRP-conjugated secondary Abs provides a colorimetric readout that is quantified by spectrophotometry equipped with SoftMax Pro software (Molecular Devices, Sunnyvale, CA).

## Immunoblot analysis

Cell lysate proteins were solubilized with 25 mM Tris, 192 mM Glycerine and 0.1% SDS buffer (Bio-Rad, Hercules, CA) and electrophoresed on a 10% or 4–12 % Tris-Glycine gel (NuSep, Australia). Proteins were transferred onto nitrocellulose membrane and were

probed with various specific primary antibodies and then the appropriate ECL labeled secondary antibodies. Proteins were visualized by ECL (Thermo, Rockford, IL).

### Fluorimetric cytotoxicity assay

Cytotoxicity was assessed with Fluorimetric cell viability assay using CellTiter-Blue® (Promega, Madison, WI). Briefly, cells were incubated for the incubated times at 37 °C with determined doses of drugs. After washing treated cells, CellTiter-Blue® reagents (20 µl) were added to suspended cells with new complete RPMI 1640 media (80 µl) and these were incubated in 96-well plates for 4 h at 37 °C. The fluorescent signal was measured at 560<sub>Ex</sub>/590<sub>Em</sub> using a fluorescence plate reader equipped with SoftMax Pro software (Molecular Devices, Sunnyvale, CA), and the level of fluorescent resorufin was calculated. Dose-response curves were calculated based on the cell viability assay of cells treated with each chemotherapeutic drug. Cell viability was assessed based on the value of fluorescent signal of live cells with no drug treatments. And the viabilities of drug treated cells were calculated based on a ratio of the fluorescent signal using the following equation:

$$\text{Cell Viability}(\%) = V_{\max} \times \frac{S_{\alpha}}{S_0}$$

In this equation,  $V_{\max}$  is the full range of cell viability, i.e. 100%;  $S_{\alpha}$  is the value of fluorescent signal of live cells at  $\alpha$  of drug concentration; and  $S_0$  represents the value of fluorescent signal of live cells with no treatments. All assays were performed in triplicate, and data are expressed as mean values  $\pm$  standard deviation.

### IC<sub>50</sub>

IC<sub>50</sub> value (the concentration of a drug that is required for 50% inhibition *in vitro*) was used to indicate the quantitative measure of the different cell killing effect of drugs. The Hill-Slope logistic model is used to calculate IC<sub>50</sub> using CompuSyn software (ComboSyn, NJ, USA).

### Drug combination assay

The synergic cytotoxic effects of bortezomib and arsenic trioxide were determined by combination index (CI) method based on Chou and Talalay equation [20], and analyzed by the CompuSyn software (ComboSyn, NJ, USA). Briefly, Combination index (CI) equation is quantitative measure of the degree of drug interaction in term of synergism and antagonism of a given endpoint of the effect measurement [21], and the following median-effect equation [ $f_a/f_u = (D/D_m)^m$ ]; a general equation for dose-effect relationship that takes into account both the potency ( $D_m$ ) and the shape ( $m$ ) of dose-effect curve where  $f_a$  and  $f_u$  are the fractions affected and unaffected, respectively<sup>17</sup> is the basis of following CI equation:

$$\sum_{i=0}^n \frac{(D)^i}{(D_x)^i} = CI$$

In this equation,  $n$  is the number of combined drugs;  $(D_x)$   $i$  is the dose of Drug  $i$  alone that inhibits  $x\%$ ; and  $(D)$   $i$  is the portion of Drug  $i$  in drug combination also inhibits  $x\%$ . Synergy is present when the CI is less than 1.0, additive effect is when CI equals 1.0, and antagonism is when CI greater than 1.0.

## Quantitative reverse transcription-polymerase chain reaction (real time-PCR)

Messenger RNA (mRNA) samples were subjected to RNase-free DNase treatment performed according to RNeasy<sup>®</sup> Mini Kit (QIAGEN, Germantown, MD) and reverse transcribed to cDNA using SuperScript<sup>®</sup> III First-Strand Synthesis System (Invitrogen, Carlsbad, CA) as per the manufacturer's instructions. The primers were designed using the PrimerExpress software (Applied Biosystems). Quantitative reverse transcription-polymerase chain reactions (real time-PCRs) were performed using RT<sup>2</sup> SYBR<sup>®</sup> Green/ROX<sup>™</sup> qPCR Master Mix (SABiosciences, Foster City, CA) according to the manufacturer's instructions. Human  $\beta$ -actin or GAPDH genes were used as internal controls. All samples were run in duplicate using ABI 7900HT Fast Real-Time PCR System equipped with SDS Software v2.3 software (Applied Biosystems), and data were analyzed using the comparative Ct method ( $-\Delta\Delta C_t$ ).

## Statistical analysis

All assays were performed in duplicate or triplicate, and data are expressed as mean values  $\pm$  standard deviation. Statistical analyses were performed using software SPSS for Windows version 12.0. Statistical significance of differences between the cell groups was evaluated by Anova test or Student's *t*-test. *P* values  $<0.05$  were considered statistically significant.

## RESULTS

### Reduction of MCL cell growth by Arsenic trioxide (ATO)

First, the effects of ATO on cell proliferation were tested in MCL cells at several concentrations. In both Jeko-1 and SP-53 cells, ATO effectively suppressed MCL cell proliferation in a dose-dependent manner (Figure 1A). In the control (0  $\mu$ M ATO) or at the lowest concentration of ATO (1  $\mu$ M), the Jeko-1 and SP-53 cells proliferated as expected over 18–48 hours. At the lowest concentration of ATO (1  $\mu$ M), the proliferation rates of the MCL cells themselves surpassed the inhibition of growth induced by ATO. Higher ATO concentrations (more than 5  $\mu$ M), however, readily suppressed the growth of MCL cell lines (Figure 1A). MCL tumor cells from six different xenograft mice were also tested for the effects of ATO; the proliferation of xenograft tumor cells was effectively inhibited by 5  $\mu$ M of ATO (Supplemental Figure 1).

The  $IC_{50}$  of ATO was then measured using cells from several MCL patients and MCL cell lines. All patient tumor cells were collected via aphaeresis as indicated in the materials and methods. The cells ( $2 \times 10^5$  cells/ml) were incubated for 18–24 hours with concentrations of ATO ranging from 0–10  $\mu$ M. The mean  $IC_{50}$  values of ATO in primary MCL cells were comparable with those of both MCL cells lines (Figure 1B). These data demonstrate that ATO inhibit the growth of both the primary patient cells and the MCL cell lines.

### Effects of ATO on the expression of cyclin D1 in MCL

To investigate the effects of ATO at the molecular level, this study next focused on cyclin D1, an important component in cell cycle regulation and a genetic hallmark of MCL [22]. Over expressed cyclin D1, in part, contributes to uncontrolled cell proliferation in several human cancers, including MCL. ATO treatment (5  $\mu$ M) effectively reduced cyclin D1 expression within 24–48 hours compared with the untreated control (Figure 2A). The relative level of reduction as determined by real time-PCR was approximately 45–50%; however, the amount of cyclin D1 protein in MCL cells after a 48 hour treatment was undetectable (Figure 2B). These data imply that the modulation of the cell cycle factor cyclin D1 by ATO could result in delayed cell proliferation and/or lead to cell death.

## Induction of MCL cell apoptosis by ATO

To further clarify the molecular mechanisms of the cell growth inhibition by ATO, MCL cell apoptosis was measured using Annexin V and 7-AAD. After a 48 hour treatment with ATO, the percentage of dead cells (upper right quadrant) gradually increased from 9.6% to 71.9% in a dose-dependent manner compared with the percentage of dead MCL cells without ATO treatment (Figure 3A). Early apoptotic cells, which are Annexin V positive and 7-AAD negative (lower right quadrant), were slightly decreased when the cells advanced to the late stage of apoptosis (Figure 3A).

The increased number of late apoptotic cells (Annexin V positive and 7-AAD positive cells) after ATO treatment correlated with the decreased levels of the cell survival factor, Bcl-2 (Figure 3B). Interestingly, Bcl-2 mRNA levels were not decreased compared with controls after a 24 hour treatment, indicating that the majority of cells are alive or in an early apoptotic stage. The decrease in Bcl-2 gene expression after ATO treatment was confirmed by immunoblot analyses. Compared with the GAPDH control, both MCL cells displayed decreased levels of Bcl-2 protein expression after ATO treatment (Figure 3C).

Next, the effects of ATO on the expression of caspase-3 and -9, members of the caspase family that play central roles in cell apoptosis, were examined. Immunohistochemistry analyses showed that the majority of MCL cells express activated caspase-3 and -9 after ATO treatment for 48 hours (Figure 3D). The effects of ATO on the expression of cleaved poly(ADP-ribose) polymerase (PARP) were then investigated. During chemotherapeutic drug-induced apoptosis in a variety of cancer cells, PARP is cleaved into 89- and 24-kDa fragments that contain the active site and DNA-binding site, respectively [23–25]. Caspase 3 has been shown to be mainly responsible for the cleavage of the PARP protein during programmed cell death [23–25]. ATO treatment for 48 hours greatly increased the levels of PARP in the cells (Figure 3E). In conclusion, these data indicate that ATO treatment induces cell apoptosis in MCL cells via modulation of cell cycle components that are concomitant with increased apoptotic factors.

Constitutive NF- $\kappa$ B expression has been known to contribute to increased cell survival in several hematological malignancies and in stem cells in hematological cancers [26–28]. Because we previously showed that NF- $\kappa$ B plays important roles in cell survival in MCL [17], the levels of NF- $\kappa$ B components after ATO treatment were investigated. Two main NF- $\kappa$ B components constitutively expressed in MCL cells, p50 and p65, showed relatively reduced DNA binding activities by ELISA assay after ATO treatment (Figure 4A). Several NF- $\kappa$ B downstream target genes, such as IL-6, IL-8, and c-IAP2, were also reduced as determined by real time-PCR [28] (Figure 4B). These data demonstrate that ATO can suppress constitutive NF- $\kappa$ B expression in MCL, which in turn, further down-regulates cell survival pathways.

## ATO synergizes with the cytotoxic effect of bortezomib in MCL cells

Because most chemotherapeutic agents are used in a combined regimen, we investigated whether ATO can modulate the effects of existing drugs used in MCL. We tested cell survival rates in MCL cells after bortezomib treatment with or without ATO. The combination of ATO with bortezomib largely increased cell cytotoxicity in Jeko-1 and SP-53 MCL cells compared with bortezomib alone (Figure 5A). To test the effects of ATO on bortezomib resistance, the bortezomib-resistant MCL cell lines, Mino and Rec-1, were used. Compared with bortezomib treatment without ATO, the combination of bortezomib with ATO induced higher levels of cytotoxicity in the bortezomib-resistant cell lines, Mino and REC-1 (Figure 5A). After adding ATO, the IC<sub>50</sub> values of bortezomib were markedly decreased in bortezomib-resistant Mino and REC-1 cells as well as in bortezomib-sensitive

Jeko-1 and SP-53 cells (Figure 5B). Combination index (CI) plots by the Chou-Talalay method supported the observation that ATO had synergistic cytotoxic effects with bortezomib not only in bortezomib-sensitive, but also in bortezomib-resistant MCL cells (Figure 5C).

The effects of ATO treatment with bortezomib were also investigated in primary MCL cells. In all tested MCL primary cells, the cytotoxicity rates after a combination treatment of bortezomib and ATO were much higher than after treatment with bortezomib alone (Figure 6A). The IC<sub>50</sub> values of bortezomib after ATO addition were 60–90% lower than those of bortezomib alone (Figure 6B). These data suggest that bortezomib can be used in lower doses when used in combination with ATO and still achieve a similar degree of cytotoxicity as higher doses. Most of the patient cells showed a CI value of less than 1, indicating that ATO effectively synergized with bortezomib to induce cytotoxicity in MCL cells (Figure 6C).

## DISCUSSION

Arsenic trioxide (As<sub>2</sub>O<sub>3</sub>, ATO) has been used as a therapeutic drug for thousands of years in Chinese medicine [4]. Medicinal trials were, however, discontinued in the mid-20<sup>th</sup> century due to links to skin cancer and after that, it was generally accepted as a potent environmental carcinogen [29]. Later studies discovered that both arsenic trioxide and arsenic sulfide induce complete remission (CR) in both primary and relapsed acute promyelocytic leukemia [5]. The mechanism of action for ATO is different depending on the concentration; ATO triggers apoptosis at high concentrations (more than 5 μmol/L) and induces cell differentiation, which could be related to retinoic acid signaling [30], at low concentrations (0.1 to 0.5 μmol/L). Several clinical trials showed that ATO administration can be effective as a single agent in treating multiple myeloma (MM) and myelodysplastic syndromes (MDS) [9,10], although the reported success rates were not as promising as those observed in APL. In contrast, there were disappointing clinical results with ATO in non-APL acute myeloid leukemia (AML) [31].

The survival rate of MCL is one of the lowest among NHLs. Conventional and newer therapeutic strategies, including antibody-based therapies, are not effective in high-grade and relapsed MCL, suggesting alternative therapeutic strategies are highly desired. Given that ATO shows some effectiveness in multiple myeloma [8], we hypothesized that testing the effects of ATO in MCL was worthwhile.

ATO triggered apoptosis at a relatively low concentration in MCL cells (Figure 1). The growth of cells treated with ATO was significantly compromised compared with treatment without ATO (Figure 1A). ATO triggered the apoptotic program, particularly by increasing the levels of apoptotic molecules such as caspase-3, -9 and cleaved PARP (Figures 3D and 3E). PARP-1 is cleaved by caspase-3 or -7 during apoptosis, further activating the apoptotic program [20]. The cleavage of PARP-1, which occurs between Asp214 and Gly215, results in the separation of the two zinc finger DNA-binding motif in the NH<sub>2</sub> terminal region of the enzyme. Cleaved PARP has also been suggested to prevent further repair of DNA strand breaks during the apoptosis [32,33]. ATO treatment in MCL also decreased the levels of cyclin D1, which plays an important role in uncontrolled MCL proliferation (Figures 2A and 2B). Constitutive expression of NF-κB has been reported in several cancers including MCL [16]. In this study, we showed ATO effectively suppressed NF-κB expression and the downstream signaling pathways linked to NF-κB. In addition, IL-6, IL-8 and c-IAP2 mRNA levels were all down regulated upon ATO treatment (Figures 4A and 4B).

Bortezomib has been used to treat MM and was recently approved for treating MCL. Because the constitutive NF- $\kappa$ B signaling pathway is affected by ATO treatment, we decided to test the effect of combining ATO with bortezomib. The expression of the constitutive NF- $\kappa$ B signaling axis increases the survival of malignant stem cells in leukemia and MCL [17,28]. ATO synergized the antiproliferative effects of bortezomib at relatively low concentrations in primary MCL cells and in MCL cell lines (Figures 5 and 6). A lower concentration of bortezomib with ATO achieved rates of cell cytotoxicity similar to that of a higher concentration of bortezomib alone (Figures 5B and 6B).

ATO also effectively suppressed the growth rate of bortezomib-resistant MCL cells. The combination of bortezomib and ATO increased cell cytotoxicity in Mino and Rec-1 cells, which are bortezomib-resistant (Figure 5). These data suggest that ATO combination therapies could be an effective therapeutic alternative to lower the toxicity of bortezomib, with further clinical testing required to prove its efficacy.

In conclusion, this study demonstrates the effect of ATO on the hematologic malignancy of MCL. A previous study also shows that ATO can induce apoptosis in MCL cell lines via increased levels of cleaved caspases [34]. Together, these findings suggest that ATO is a worthwhile alternative option for MCL treatment and provide preclinical evidence supporting a new combination regimen of bortezomib and ATO to overcome the bortezomib resistance of MCL.

## Supplementary Material

Refer to Web version on PubMed Central for supplementary material.

## Acknowledgments

The tissue samples were provided by the University of Texas M. D. Anderson Cancer Center Satellite Lymphoma Tissue Bank which was supported by Institutional Core Grant # NCI/NIH - CA16672. This work is funded by CONquer canCER Now award (CONCERN Foundation) and NCI/NIH grant given to NM.

## REFERENCES

1. Mounter PJ, Lennard AL. Management of non-Hodgkin's lymphomas. *Postgraduate Medical Journal*. 1999; 75:2–6. [PubMed: 10396578]
2. Salaverria I, Perez-Galan P, Colomer D, Campo E. Mantle cell lymphoma: from pathology and molecular pathogenesis to new therapeutic perspectives. *Haematologica*. 2006; 91:11–16. [PubMed: 16434365]
3. Pileri SA, Falini B. Mantle cell lymphoma. *Haematologica*. 2009; 94:1488–1492. [PubMed: 19880776]
4. Bonati A, Rizzoli V, Lunghi P. Arsenic trioxide in hematological malignancies: The new discovery of an ancient drug. *Curr Pharm Biotechnol*. 2006; 7:397–405. [PubMed: 17168655]
5. Douer D, Tallman MS. Arsenic trioxide: New clinical experience with and old medication in hematological malignancies. *J. Clin. Oncol*. 2005; 33:2396–2410. [PubMed: 15800332]
6. Chen GQ, Zhu J, Shi XG, Ni JH, Zhong HJ, et al. In vitro studies on cellular and molecular mechanisms of arsenic trioxide (As<sub>2</sub>O<sub>3</sub>) in the treatment of acute promyelocytic leukemia: As<sub>2</sub>O<sub>3</sub> induces NB4 cell apoptosis with downregulation of Bcl-2 expression and modulation of PML-RAR alpha/PML proteins. *Blood*. 1996; 88:1052–1061. [PubMed: 8704214]
7. Zhang TD. Treatment of acute granulocytic leukemia with Ai ling No. 1: clinical analysis and experiment research. *Chin. J. Comb. Trad. West Med*. 1984; 4:19–20.
8. Rollig C, Illmer T. The efficacy of arsenic trioxide for the treatment of relapsed and refractory multiple myeloma: A systemic review. *Cancer Treatment Review*. 2009; 35:425–430.



9. Munshi NC, Tricot G, Desikan R, Badros A, Zangari M, Toor A, Morris C, Anaissie E, Barlogie B. Clinical activity of arsenic trioxide for the treatment of multiple myeloma. *Leukemia*. 2002; 16:1518–1521.
10. Hussein MA, Saleh M, Ravandi F, Mason J, Rifkin R, Eliason R. Phase 2 study of arsenic trioxide in patients with relapsed or refractory multiple myeloma. *Br. J. Haematol*. 2004; 125:470–476. [PubMed: 15142117]
11. Ravandi F. Arsenic trioxide: expanding roles for an ancient drug? *Leukemia*. 2004; 18:1457–1459. [PubMed: 15269784]
12. Miller WH, Shipper HM, Lee JS, Singer J, Waxman S. Mechanisms of action of arsenic trioxide. *Cancer Res*. 2002; 62:3893–3903. [PubMed: 12124315]
13. Huang XJ, Wiernik PH, Klein RS, Gallagher RE. Arsenic trioxide induces apoptosis of myeloid leukemia cells by activation of caspases. *Medical Oncology*. 1999; 16:58–64. [PubMed: 10382944]
14. Decker P, Muller S. Modulating poly (ADP-Ribose) polymerase activity: potential for the prevention and therapy of pathogenic situations involving DNA damage and oxidative stress. *Curr. Pharma. Biotech*. 2002; 3:275–283.
15. Zhang W, Ohnishi K, Shigeno K, Fujisawa S, Naito K, Nakamura S, Takeshita K, Takeshita A, Ohno R. The induction of apoptosis and cell cycle arrest by arsenic trioxide in lymphoid neoplasms. *Leukemia*. 1998; 12:1383–1391. [PubMed: 9737686]
16. Pham LV, Tamayo AT, Yoshimura LC, Lo P, Ford RJ. Inhibition of constitutive NF-kappa B activation in mantle cell lymphoma B cells leads to induction of cell cycle arrest and apoptosis. *J Immunol*. 2003; 171:88–95. [PubMed: 12816986]
17. Jung HJ, Chen Z, Fayad L, Wang F, Romaguera J, Kwak LW, McCarty N. Bortezomib resistant nuclear factor kappa B expression in stem-like cells in mantle cell lymphoma. *Experimental Hematology*. 2011 Accepted for publication.
18. Rizzatti EG, Mora-Jensen H, Weniger MA, et al. Noxa mediates bortezomib induced apoptosis in both sensitive and intrinsically resistant mantle cell lymphoma cells and this effect is independent of constitutive activity of the AKT and NF-kappaB pathways. *Leuk Lymphoma*. 2008; 49:798–808. [PubMed: 18398749]
19. Zheng C, Ayala P, Wang M, Fayad L, Katz R, Romaguera JE, Caraway N, Neelapu SS, Kwak L, Simmons PJ, McCarty N. Identification of clonogenic mantle cell lymphoma initiating cells. *Stem Cell Research*. 2010; 5:212–225. (2010). [PubMed: 20851072]
20. Chou TC, Talalay P. Quantitative analysis of dose-effect relationships: the combined effects of multiple drugs or enzyme inhibitors. *Adv Enzyme Regul*. 1984; 22:27–55. [PubMed: 6382953]
21. Chou TC, Talalay P. Generalized equations for the analysis of inhibitions of Michaelis-Menten and higher-order kinetic systems with two or more mutually exclusive and nonexclusive inhibitors. *Eur J Biochem*. 1981; 115:207–216. [PubMed: 7227366]
22. Bertoni F, Rinaldi A, Zucca E, Cavalli F. Update on the molecular biology of mantle cell lymphoma. *Hematol. Oncol*. 2006; 24:22–27. (2006). [PubMed: 16402392]
23. Lazebnik YA, Kaufmann SH, Desnoyers S, Poirier GG, Earnshaw WC. Cleavage of poly(ADP-ribose) polymerase by a proteinase with properties like ICE. *Nature*. 1994; 371:346–347. [PubMed: 8090205]
24. Tewari M, Quan L, O'Rourke K, Desnoyers S, Zeng Z, Beidler DR, Poirier GG, Salvesen GS, Dixit VM. Yama/CPP32 beta, a mammalian homolog of CED-3, is a CrmA-inhibitable protease that cleaves the death substrate poly(ADP-ribose) polymerase. *Cell*. 1995; 81:801–809. [PubMed: 7774019]
25. Germain M, Affar EB, D'Amours D, Dixit VM, Salvesen GS, Poirier GG. Cleavage of automodified poly(ADP-ribose) polymerase during apoptosis. Evidence for involvement of caspase-7. *J. Biol. Chem*. 1999; 274:28379–28384. [PubMed: 10497198]
26. Packham G. The role of NF-kappaB in lymphoid malignancies. *Br J Haematol*. 2008; 143:3–15. [PubMed: 18573107]
27. Naugler WE, Karin M. NF-kappaB and cancer-identifying targets and mechanisms. *Curr Opin Genet Dev*. 2008; 18:19–26. [PubMed: 18440219]

28. Guzman ML, Neering SJ, Upchurch D, Grimes B, Howard DS, Rizzieri DA, et al. Nuclear factor-kappaB is constitutively activated in primitive human acute myelogenous leukemia cells. *Blood*. 2001; 98:2301–2307. [PubMed: 11588023]
29. Antman KH. Introduction: The history of arsenic trioxide in cancer therapy. *Oncologist*. 2001; 6:1–2. [PubMed: 11331433]
30. Shen ZX, Chen GQ, Ni JH, Li XS, Xiong SM, Qui QY, Zhu J, Tang W, Sun GL, Yang KQ, Chen Y, Zhou L, Fang ZW, Wang YT, Ma J, Zhang P, Zhange TD, Chen SJ, Chen Z, Wang ZY. Use of arsenic trioxide (As<sub>2</sub>O<sub>3</sub>) in the treatment of acute promyelocytic leukemia (APL): II. Clinical efficacy and pharmacokinetics in relapsed patients. *Blood*. 1997; 89:3354–3360. [PubMed: 9129042]
31. Petrie K, Zelent A, Waxman S. Differentiation therapy of acute myeloid leukemia: past, present and future. *Curr. Opin. Hematol*. 2009; 16:84–91. [PubMed: 19468269]
32. Smulson ME, Simbulan-Rosenthal CM, Boulares AH, Yakovlev A, Stoica B, Iyer S, Luo R, Haddad B, Wang ZQ, Pang T, Jung M, Dritschilo A, Rosenthal DS. Roles of poly(ADP-ribose)ylation and PARP in apoptosis, DNA repair, genomic stability and functions of p53 and E2F-1. *Adv. Enzyme Regul*. 2000; 40:183–215.
33. Scovassi AT, Poirier GG. Poly(ADP-ribose)ylation and apoptosis. *Mol. Cell. Biochem*. 1999; 199:125–137. [PubMed: 10544961]
34. Fei AM, Mao CM, Liu JJ, Zhu J, Mi JQ. Effect of arsenic trioxide on induction of apoptosis in MCL cell line and its possible mechanisms. *Zhongguo Shi Yan Xue Ye Xue Za Zhi*. 2010; 18:909–913. [PubMed: 20723298]

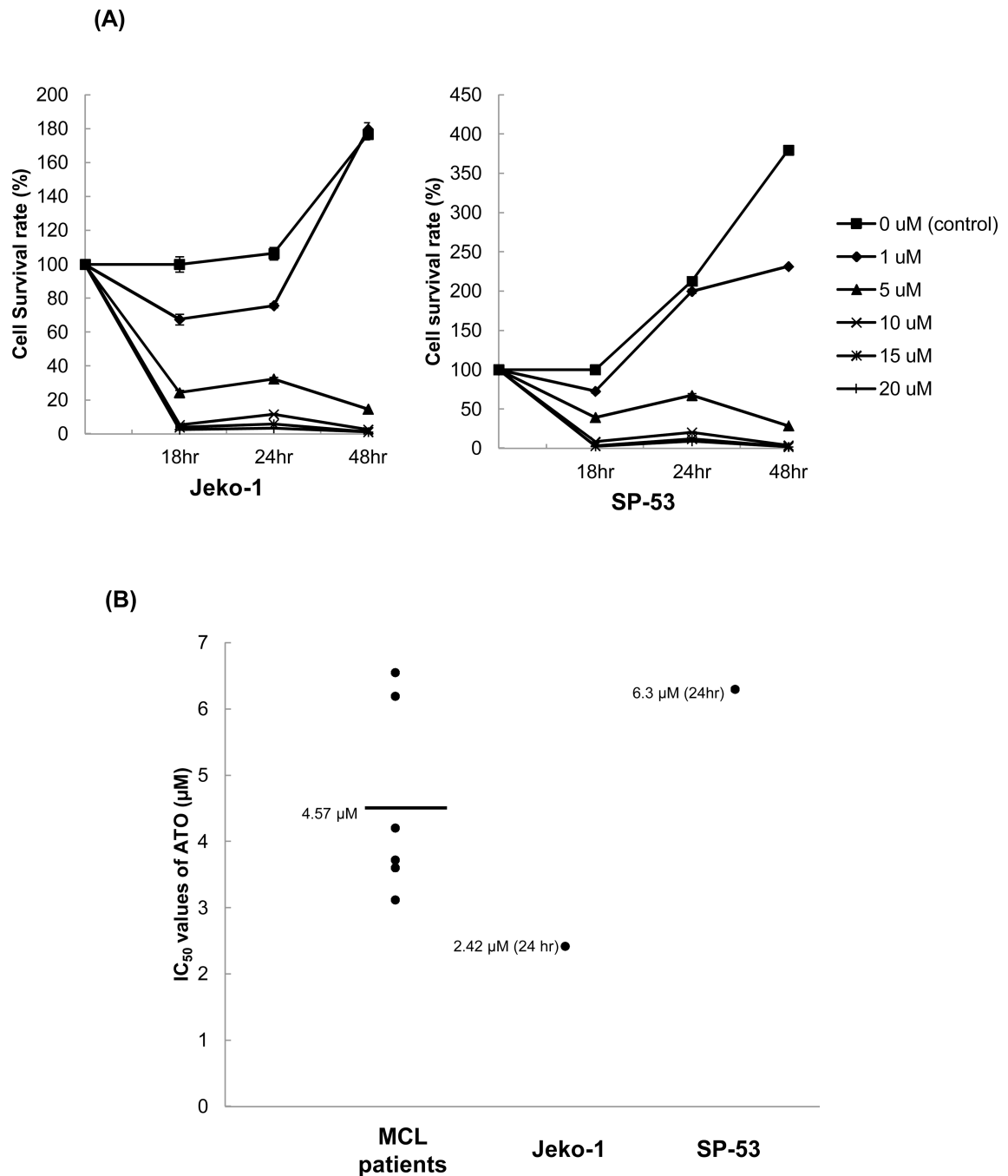
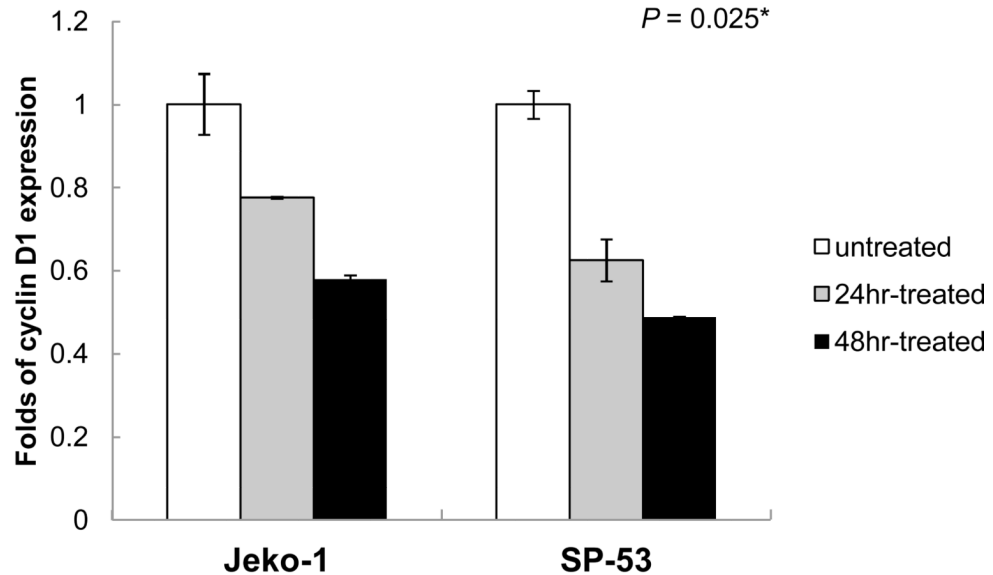


**Figure 1. Arsenic trioxide (ATO) affects the growth of MCL cells**

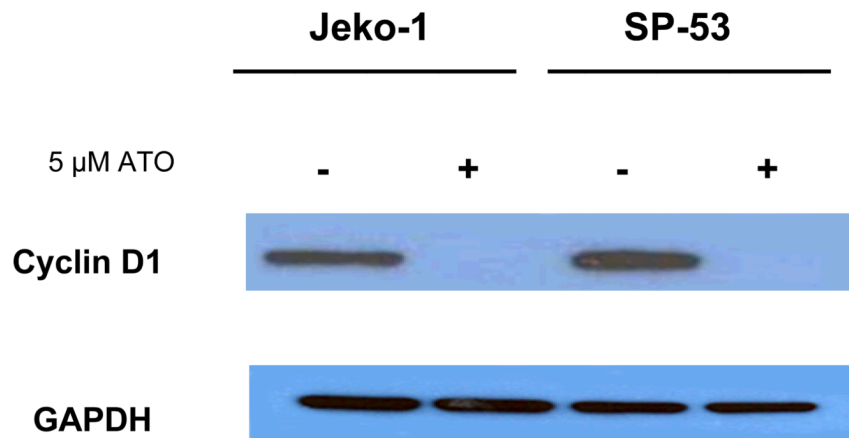
(A) ATO inhibited the proliferation of MCL cell lines in a dose- and time-dependent manner. The sensitivities of the MCL cell lines, Jeko-1 and SP-53, to ATO were determined using the CellTiter-Blue<sup>®</sup> fluorometric cell viability assay (Promega). The cells were cultured for 18, 24, and 48 hrs with different concentrations of ATO. ATO was serially diluted from a maximal dose of 20 μM. Cell viability was presented as a ratio comparing cells given treatment with those not given treatment. The results are shown as the mean ± standard deviation of triplicate experiments.

**(B)** ATO induced the cell death of primary MCL cells. MCL cells from six different patients were cultured for 18 hrs with or without ATO. ATO was serially diluted from a maximal dose of 10  $\mu$ M. The cytotoxicity of ATO was determined using the CellTiter-Blue<sup>®</sup> fluorometric assay and was presented as a ratio comparing cells given treatment with those not given treatment. The mean IC<sub>50</sub> value of ATO for primary MCL cells was comparable with the IC<sub>50</sub> values of the MCL cell lines, Jeko-1 and SP-53. The bar represents the average of IC<sub>50</sub> value of ATO for primary MCL cells.

(A)



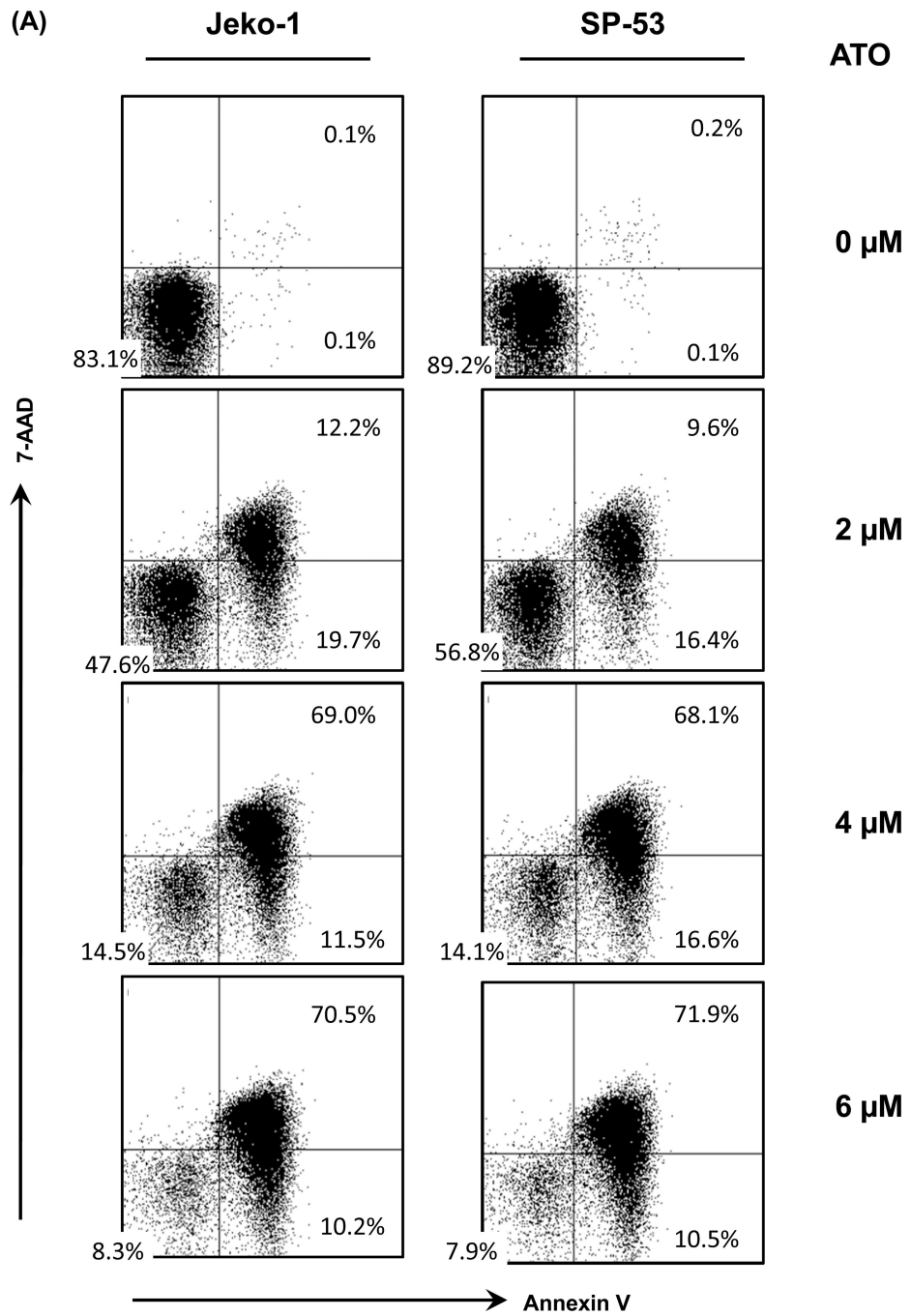
(B)

**Figure 2. ATO modulates the cyclin D1 expression in MCL**

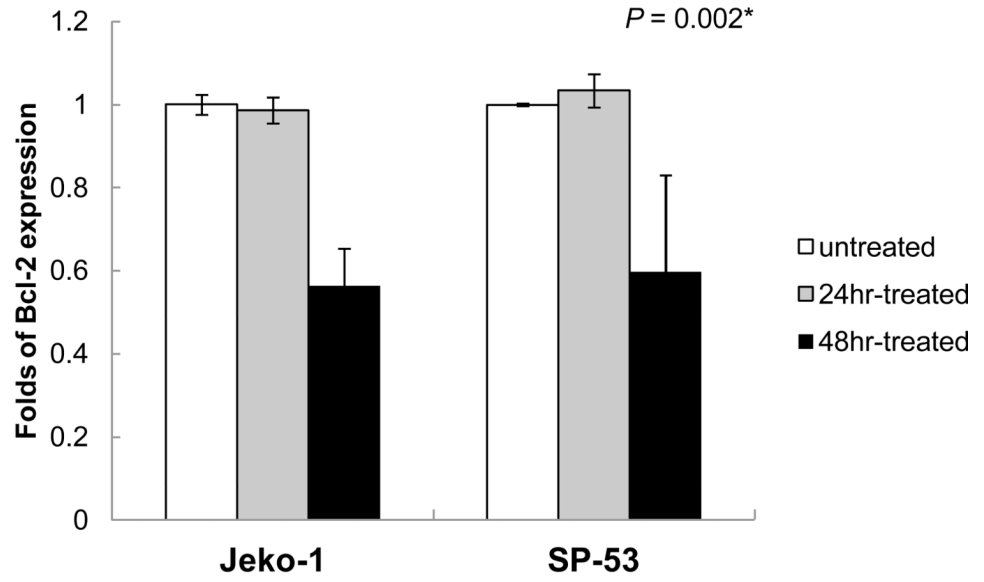
(A) ATO down-regulated the expression of cyclin D1 in MCL. The MCL cell lines, Jeko-1 and SP-53, were incubated with 5  $\mu$ M ATO for 24 or 48 hrs, after which mRNA was isolated and cDNA prepared. The cDNA was analyzed for the presence of cyclin D1 genes by real time-PCR with GAPDH used as a control. The results are shown as the mean  $\pm$  standard deviation of triplicate experiments. *P* values were calculated using the ANOVA test. \*, *P*<0.05.

(B) Jeko-1 and SP-53 cells were treated with or without 5  $\mu$ M ATO for 48 hrs. Immunoblot analyses of cyclin D1 expression were performed using cell lysate proteins from untreated

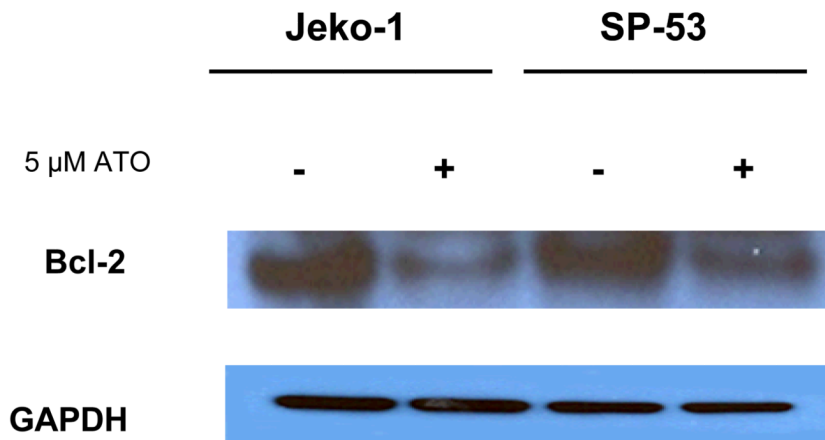
and treated Jeko-1 and SP-53 cells. GAPDH was used as a control. ATO readily suppressed the over-expression of cyclin D1 protein in MCL cells.



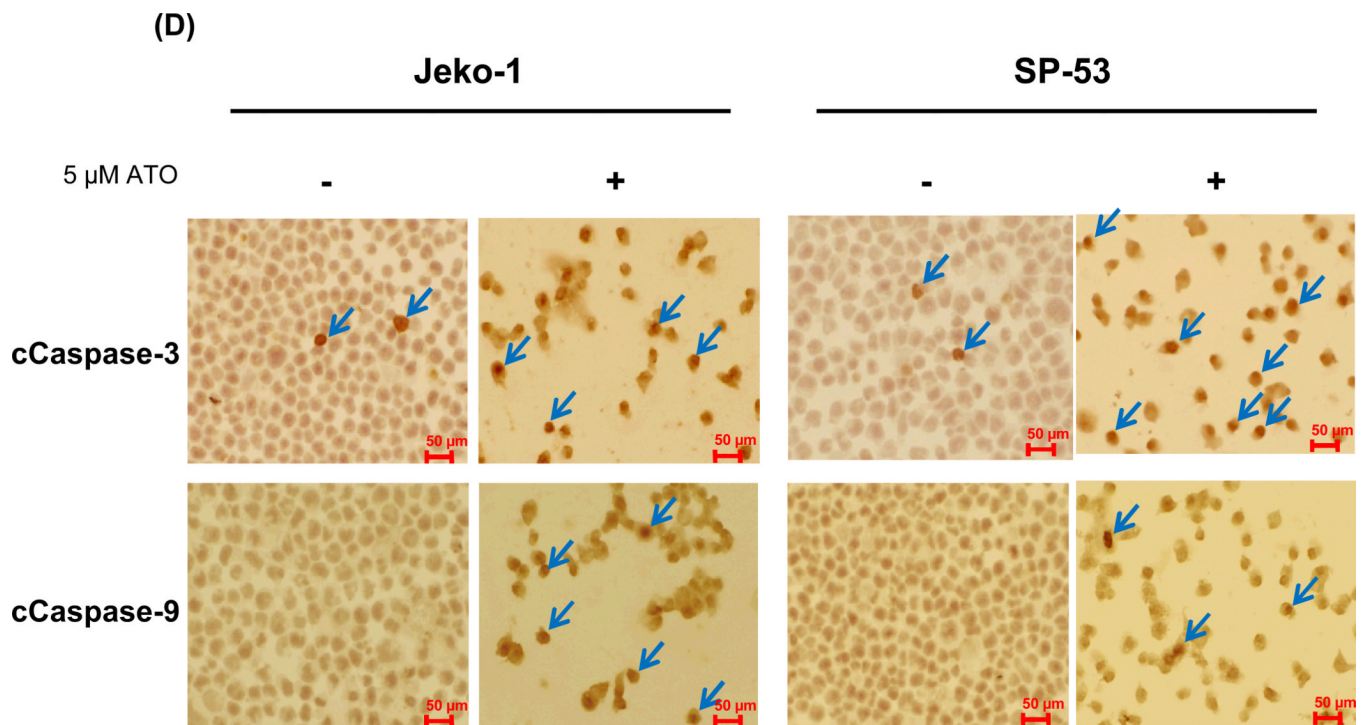
(B)



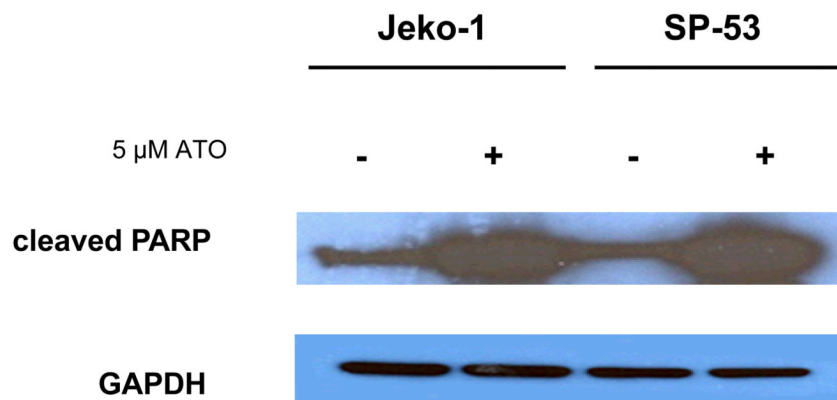
(C)







(E)

**Figure 3. ATO induces the apoptosis of MCL cells**

(A) ATO induced the dose-dependent apoptosis of MCL cells. Representative flow cytometric profiles show 7-AAD- and Annexin V-stained MCL cell lines (Jeko-1 and SP-53), after incubation with different concentrations of ATO for 48 hrs. ATO was serially diluted from a maximal dose of 6  $\mu$ M. Cells negative for both Annexin V- and 7-AAD negative cells are viable (lower left quadrant). As apoptosis proceeds, the cells become Annexin V positive and 7-AAD negative (lower right; early apoptosis) and then both Annexin V and 7-AAD positive (upper right quadrant; end stage apoptosis). The results shown are representative of at least two comparable experiments.

(B) ATO down-regulated Bcl-2-targeted gene expression in MCL. Jeko-1 and SP-53 cells were treated with 5  $\mu$ M ATO for 24 or 48 hrs. mRNA was then isolated, and cDNA was prepared for real time-PCR analysis. The cDNA was analyzed for the presence of Bcl-2 target genes, with GAPDH as a control. The results are shown as the mean  $\pm$  standard

deviation of triplicate experiments. *P* values were calculated using the ANOVA test. \*, *P*<0.05.

**(C)** Immunoblot analyses of Bcl-2, an anti-apoptotic protein, expression were performed using cell lysates from untreated and treated Jeko-1 and SP-53 cells. Jeko-1 and SP-53 cells were treated with 5  $\mu$ M ATO for 48 hrs. GAPDH was used as a control. ATO suppressed the Bcl-2 protein expression in MCL.

**(D)** ATO activated the cleavage of caspase-3 and -9 in MCL cell lines. Jeko-1 and SP-53 cells were treated with 5  $\mu$ M ATO for 48 hrs. The cytospin cells were then fixed and immunostained. Representative images with positive immunostaining for the anti-cleaved caspase-3 and -9 antibodies are shown. ATO-treated MCL cells expressed high levels of cleaved caspase-3 and -9 (arrows) compared with untreated cells. At least five sections from each cytospin slides were analyzed.

**(E)** ATO affected the activation of key proteins in the caspase cascade. Immunoblot analyses of cleaved PARP expression were performed using cell lysates from untreated and treated Jeko-1 and SP-53 cells. Jeko-1 and SP-53 cells were treated with 5  $\mu$ M ATO for 48 hr. GAPDH was used as a control. ATO induced the cleavage of the apoptotic-related protein, PARP, in MCL.

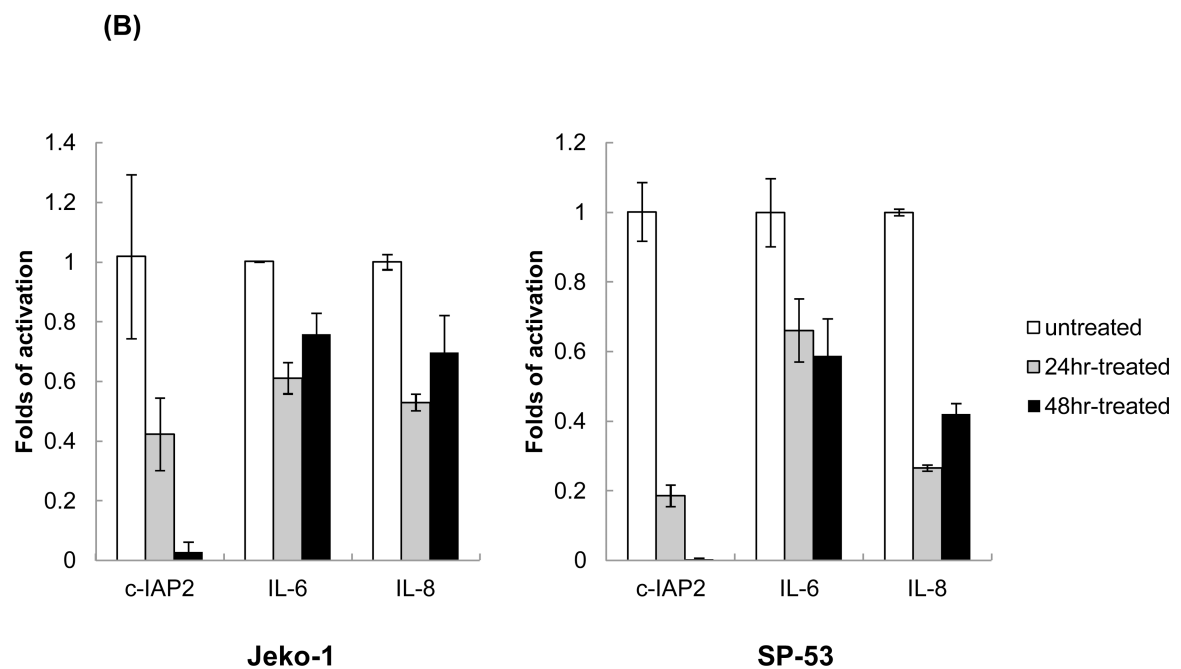
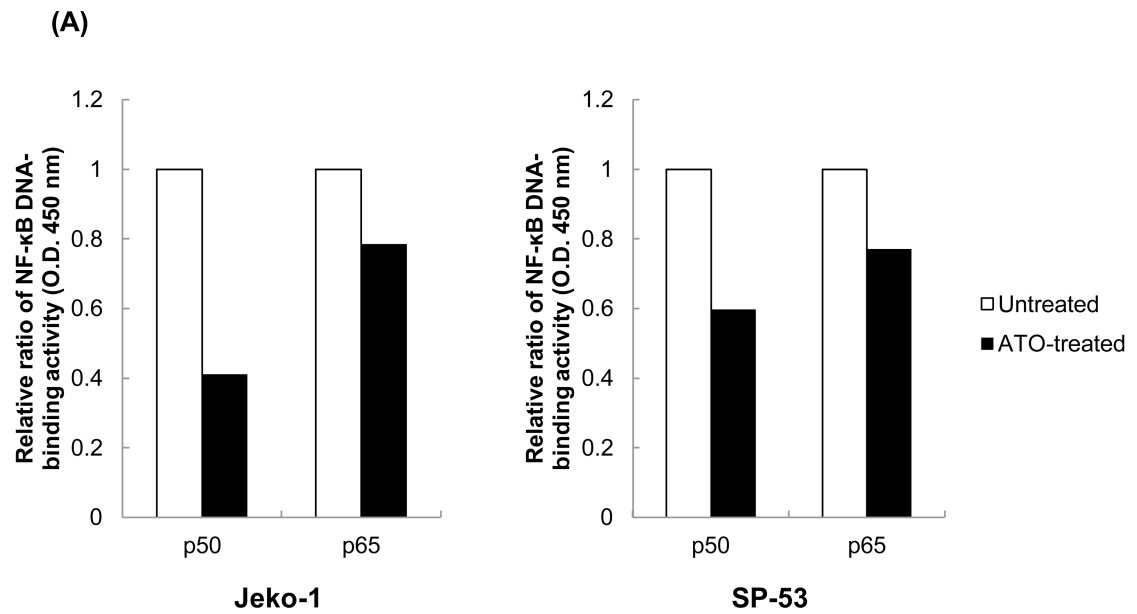
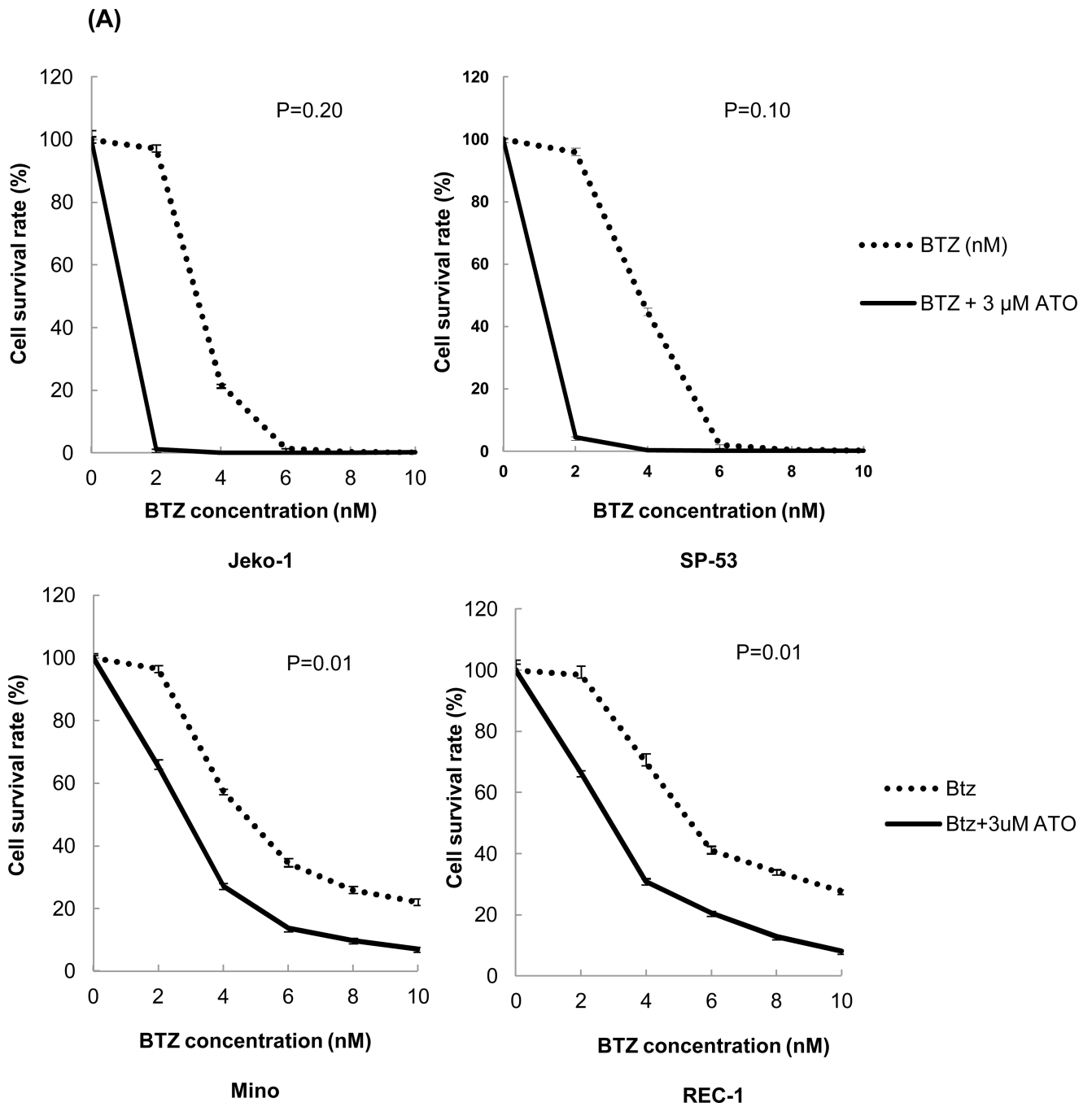


**Figure 4. ATO suppress the NF- $\kappa$ B activation in MCL cells**

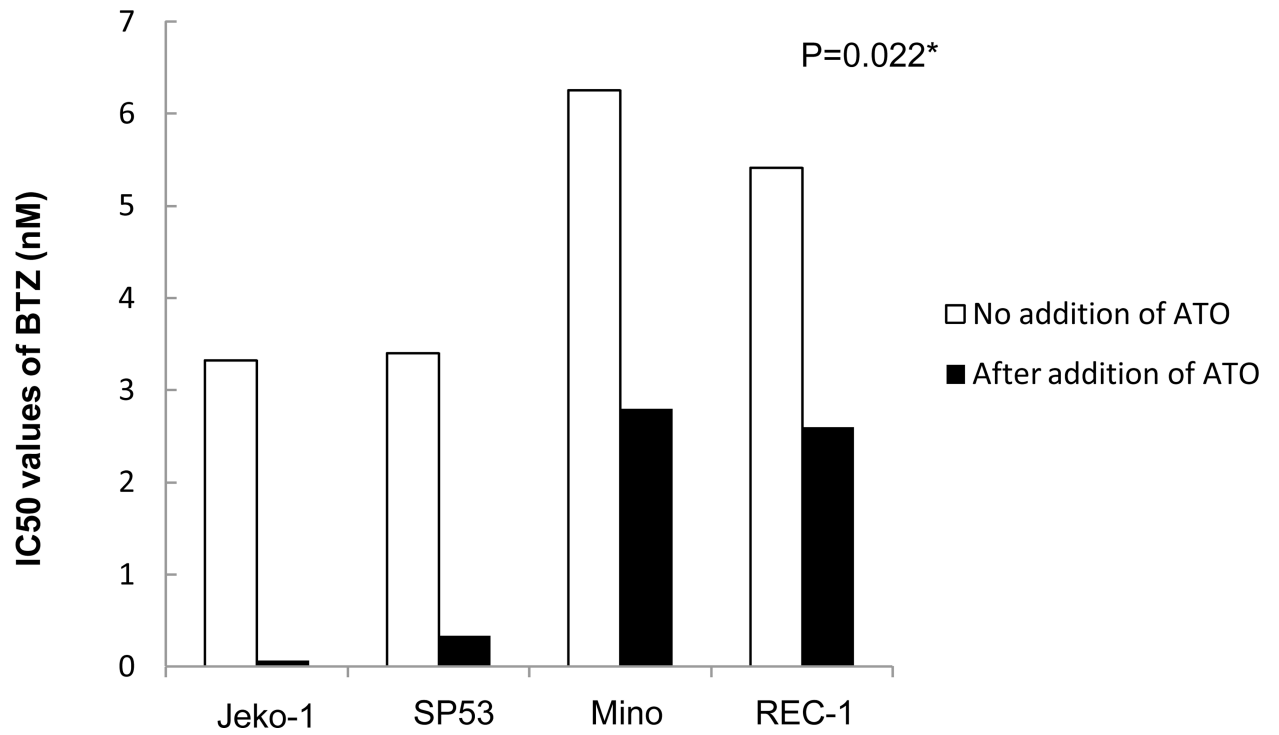
(A) NF- $\kappa$ B DNA binding activities were decreased after ATO treatment in MCL cells. Nuclear extracts from Jeko-1 and SP-53 cells that were untreated or treated with ATO (5  $\mu$ M for 24 hrs) were analyzed using ELISA assays to evaluate the DNA-binding activity of p50 and p65. Bars represent the relative ratio of p50 and p65 DNA-binding activity levels before and after treatment with ATO.

(B) Jeko-1 and SP-53 cells were cultured with 5  $\mu$ M ATO for 24 or 48 hrs. The mRNA was isolated from untreated and ATO-treated MCL cells, and then cDNA was prepared for real time-PCR. The cDNA was analyzed for the presence of genes involved in NF- $\kappa$ B-linked

transcriptional targets. GAPDH was used as a control. ATO induced the generalized suppression of the expression of the NF- $\kappa$ B target genes, IL-6, IL-8, and c-IAP2, in MCL cells. The columns are mean of duplicate experiments, and bars represent standard deviation.



(B)



(C)

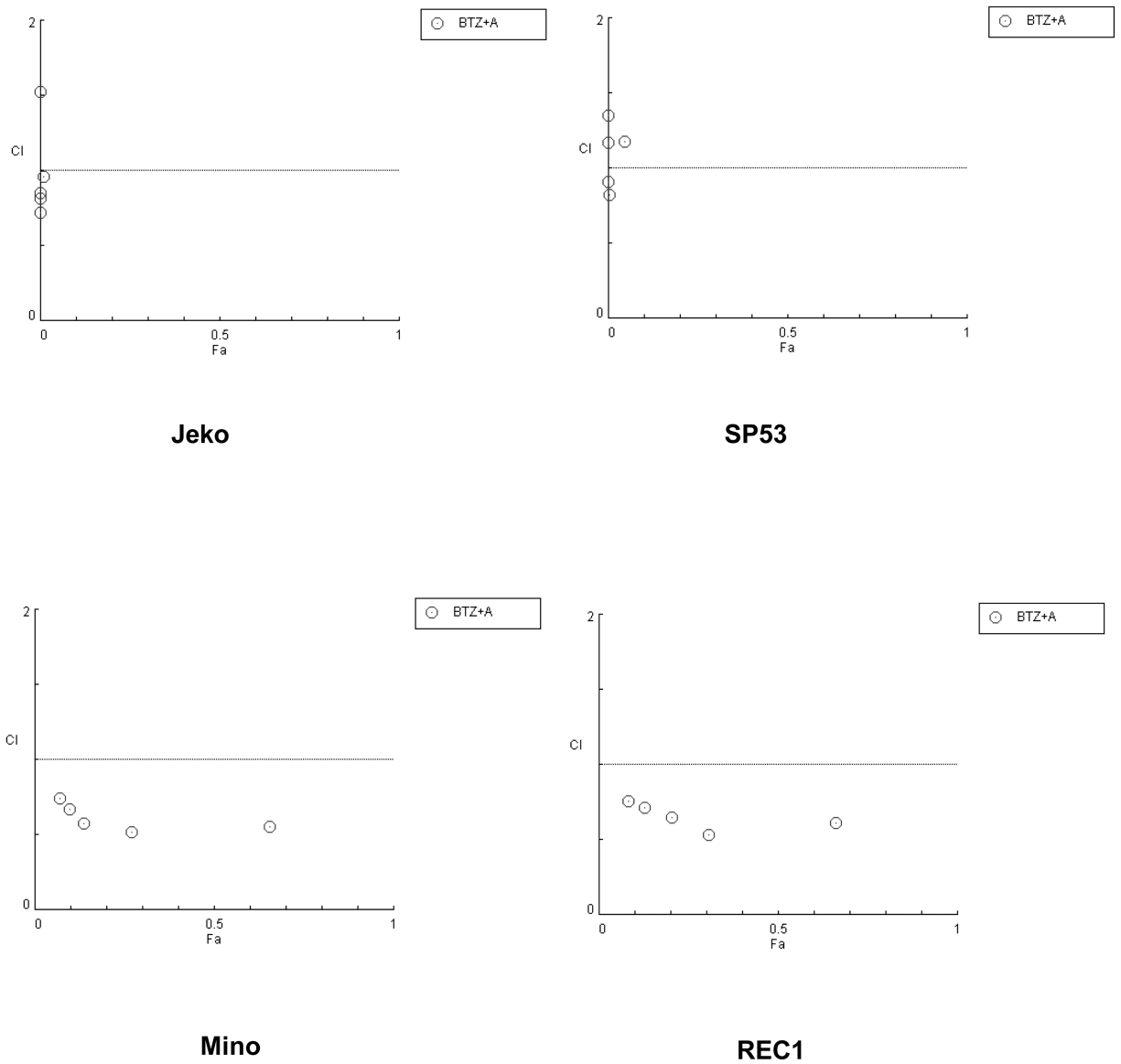


**Figure 5. ATO and bortezomib synergistically induce apoptosis in MCL cell lines**

(A) The combination of ATO and bortezomib increased the cytotoxicity of not only bortezomib-sensitive MCL cell lines, but also bortezomib-resistant MCL cell lines. Jeko-1 and SP-53 cells were used as bortezomib-sensitive MCL cell lines, and Mino, and Rec-1 cells were used as the bortezomib-resistant MCL cell lines. The cells were cultured for 24 hrs with bortezomib alone or in combination with 3  $\mu$ M ATO. Bortezomib was serially diluted as indicated. The survival rates of MCL cells treated with bortezomib alone or the combination of ATO and bortezomib were compared using the CellTiter-Blue<sup>®</sup> fluorometric cell viability assay. Cell survival rates were presented as a ratio comparing treated and

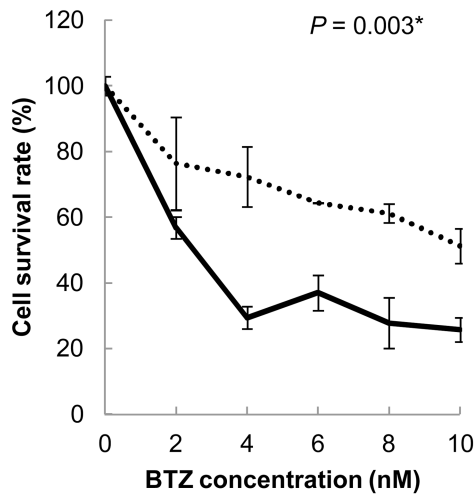
untreated cells. The results are shown as the mean  $\pm$  standard deviation of triplicate experiments. *P* values were calculated using unpaired *t*-test. \*, *P*<0.05. BTZ, bortezomib; ATO, arsenic trioxide.

**(B)** ATO markedly decreased the IC<sub>50</sub> values of bortezomib in bortezomib-resistant MCL cells and in bortezomib-sensitive MCL cells. Jeko-1, SP-53, Mino, and Rec-1 cells were cultured for 24 hrs after the addition of bortezomib with or without 3  $\mu$ M ATO. Cell viability was determined by the CellTiter-Blue<sup>®</sup> assay. The IC<sub>50</sub> values of bortezomib for all tested MCL cells were significantly decreased when in combination with ATO. \*, *P*<0.05 by unpaired *t*-test. BTZ, bortezomib; ATO, arsenic trioxide.

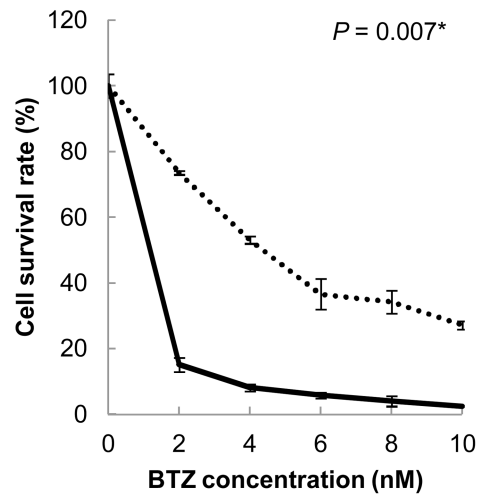
**(C)** ATO showed synergistic effects with bortezomib to induce cytotoxicity in bortezomib-resistant MCL cells and in bortezomib-sensitive MCL cells. The synergistic cytotoxic effects of bortezomib and ATO were determined using the combination index (CI) based on the data from cell viability assays. CI plots were generated using the CompuSyn software (ComboSyn, NJ, USA) according to the Chou-Talalay method. The combination of ATO and bortezomib is synergistic when CI < 1.0, additive when CI = 1, and antagonistic when CI > 1.0.



(A)

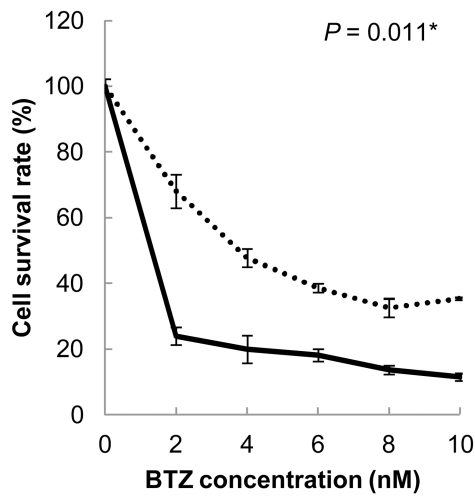


Pt1

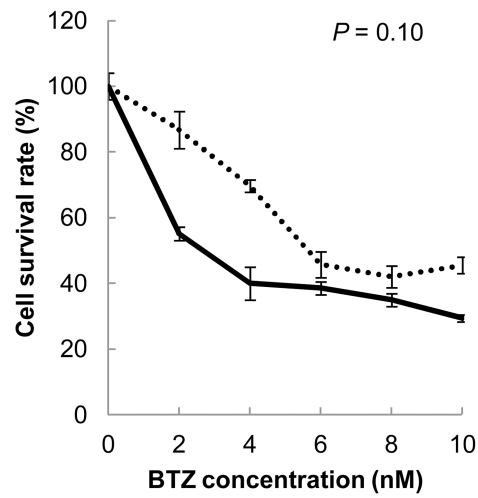


Pt2

..... BTZ alone  
 — BTZ + 3 μM ATO

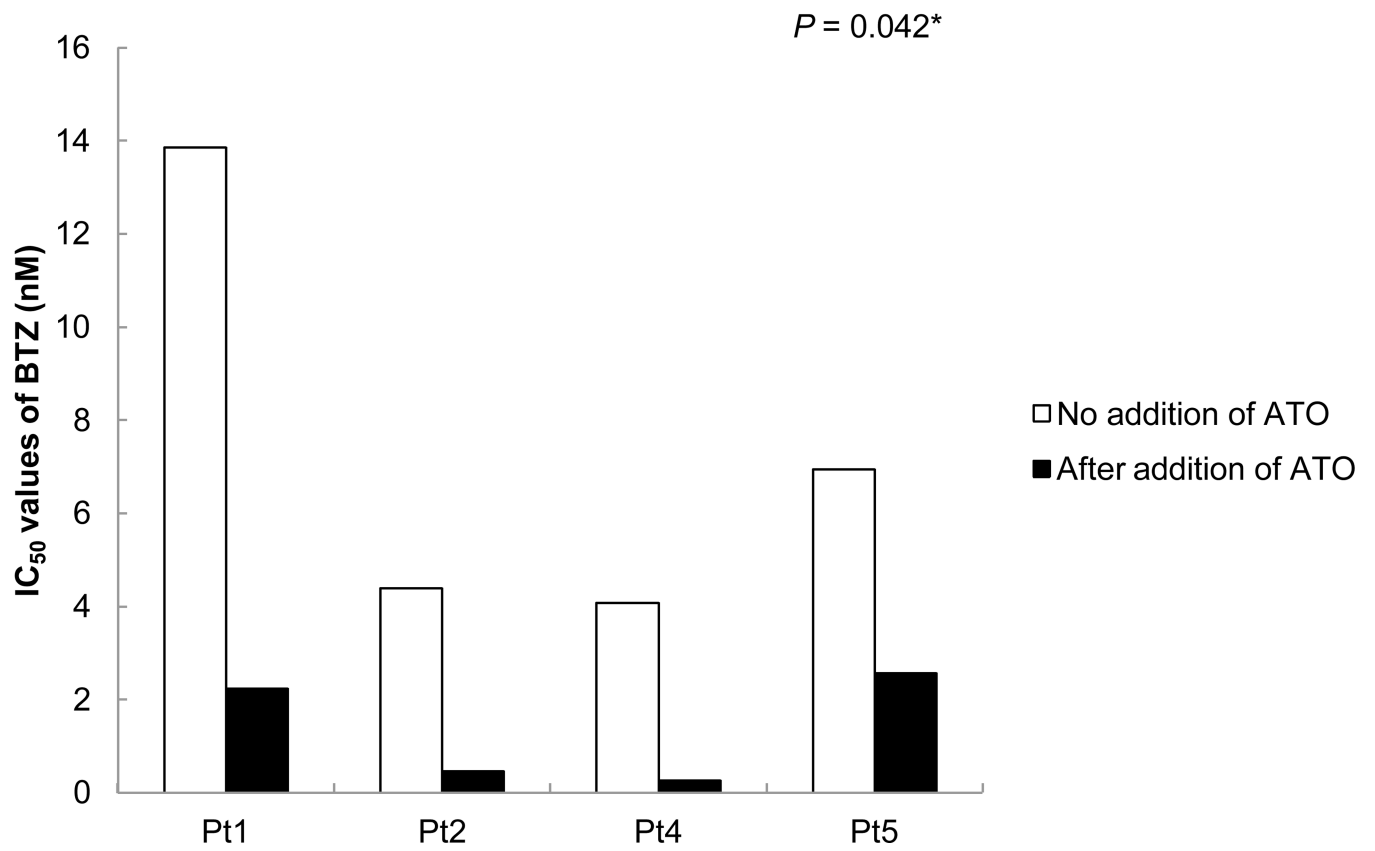


Pt4

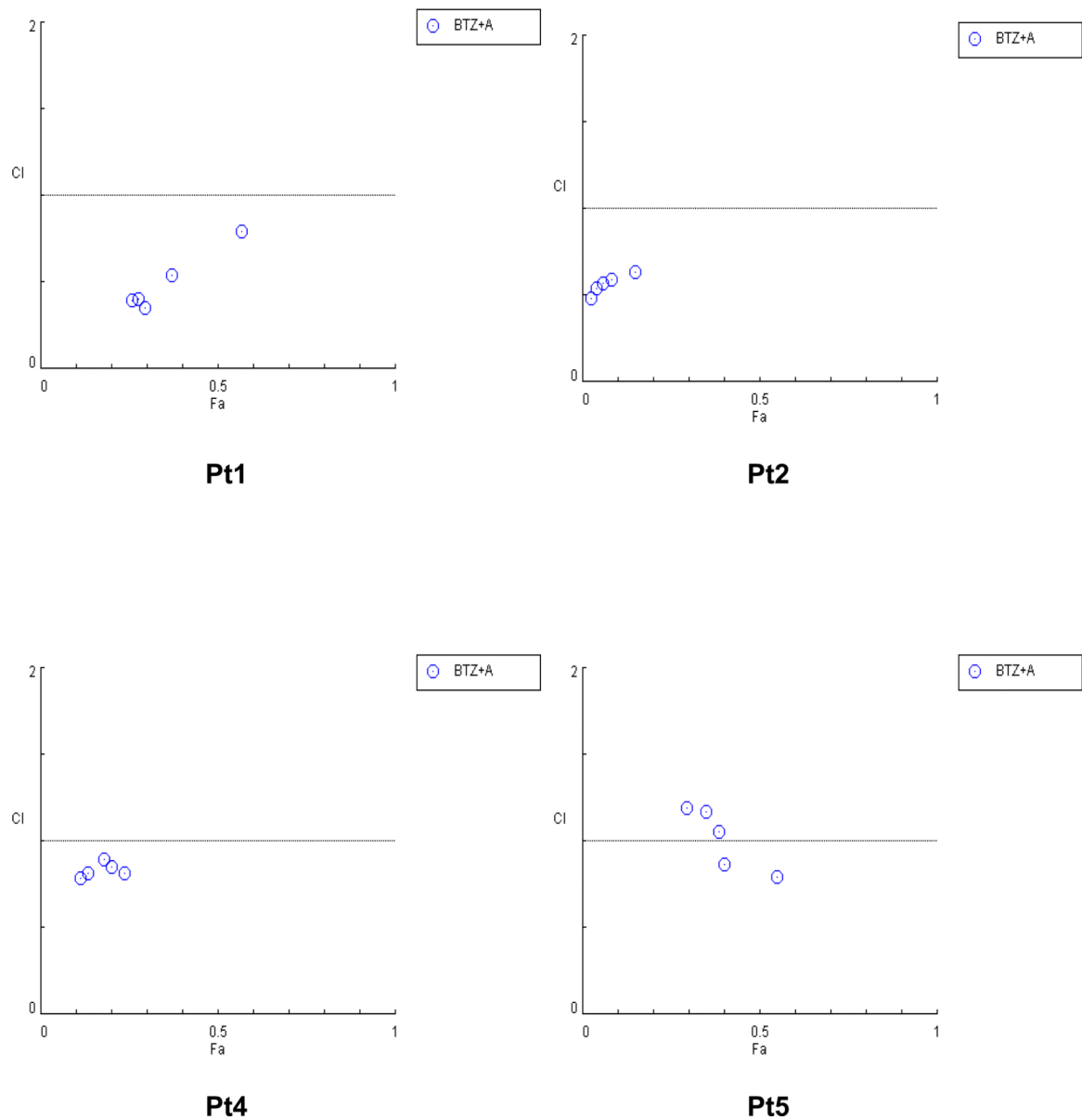


Pt5

..... BTZ alone  
 — BTZ + 3 μM ATO

**(B)**

(C)

**Figure 6. ATO sensitizes MCL patient cells to bortezomib**

(A) ATO significantly improved the bortezomib sensitivity in primary MCL cells. The chemosensitivities of MCL patient cells to bortezomib were compared with or without ATO using the CellTiter-Blue<sup>®</sup> fluorometric cell viability assay. The cells were cultured for 16 hrs with bortezomib alone or in combination with 3  $\mu$ M ATO. The drugs were serially diluted as indicated. Cell survival rates were presented as a ratio comparing treated and untreated cells. The results are shown as the mean  $\pm$  standard deviation of triplicate experiments. *P* values were calculated using the unpaired *t*-test. \*, *P*<0.05. BTZ, bortezomib; ATO, arsenic trioxide.

**(B)** ATO markedly decreased the  $IC_{50}$  values of bortezomib in MCL patient cells. Four different MCL patient samples were cultured for 16 hrs after the addition of bortezomib with or without 3  $\mu$ M ATO. Cell viability was determined by the CellTiter-Blue<sup>®</sup> assay. The  $IC_{50}$  values of bortezomib for primary MCL cells were significantly decreased when combined with ATO. \*,  $P < 0.05$  by unpaired  $t$ -test. BTZ, bortezomib; ATO, arsenic trioxide.

**(C)** ATO synergized with bortezomib to induce cytotoxicity in MCL patient samples. The synergistic cytotoxic effects of bortezomib and ATO were determined using the combination index (CI) based on the data from cell viability assays. CI plots were generated using the CompuSyn software (ComboSyn, NJ, USA) according to the Chou-Talalay method. The combination of ATO and bortezomib is synergistic when  $CI < 1.0$ , additive when  $CI = 1$ , and antagonistic when  $CI > 1.0$ .